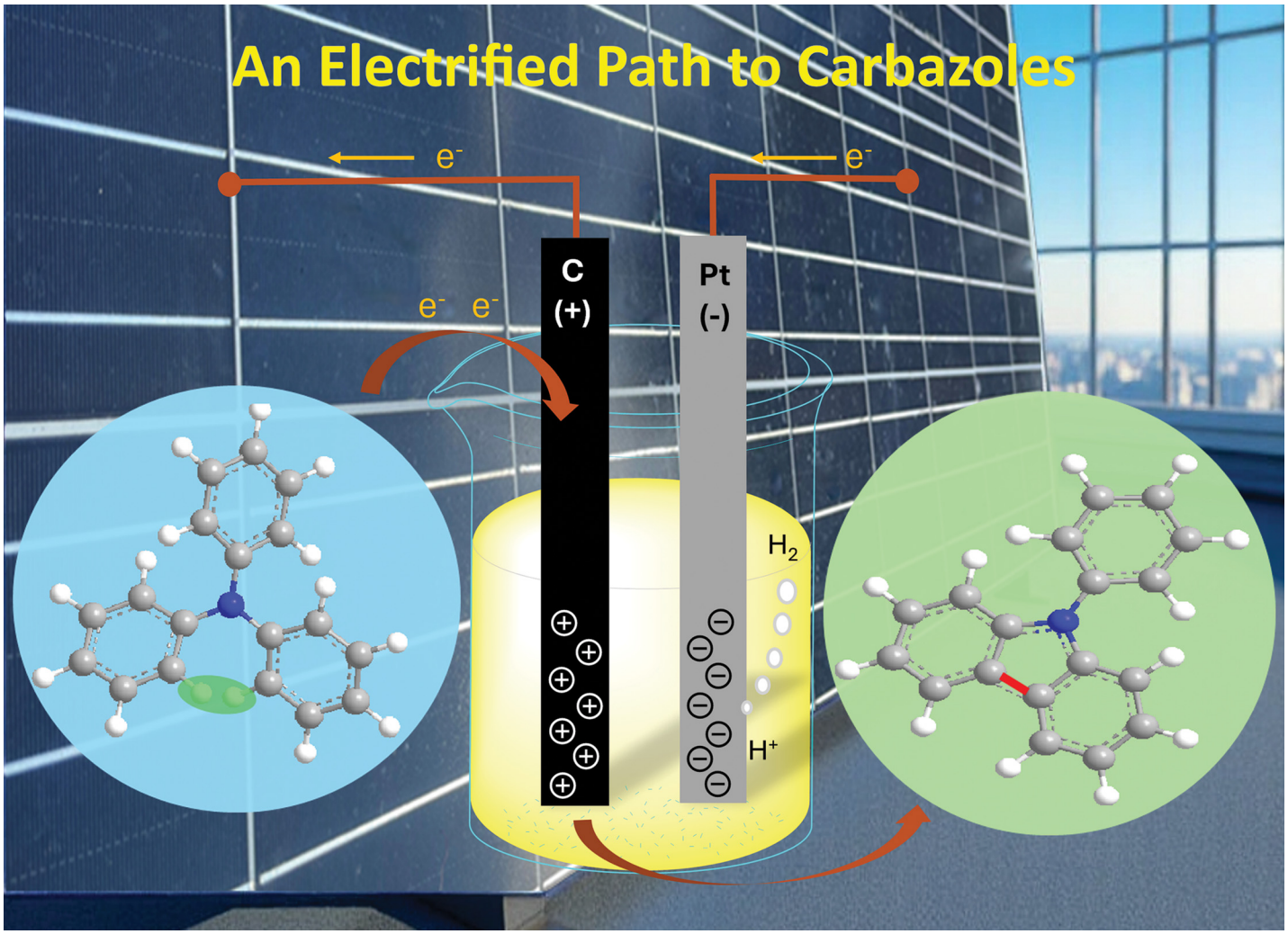

Highlighting a collaborative research effort between the Institute of Sustainability for Chemicals, Energy and Environment (A*STAR ISCE2), Singapore, and Imperial College London, United Kingdom, in advancing sustainable chemistry

Electrochemical dehydrogenative intramolecular C–C coupling for expedient carbazole synthesis

Researchers unveiled a sustainable, metal-free method to synthesise carbazoles using electricity at room temperature. The study showed the reactions are selective and follow specific patterns, offering fresh insights into greener molecular synthesis and advancing chemical innovation.

Image reproduced by permission of Balamurugan Ramalingam from *Chem. Commun.*, 2025, **61**, 14915.

As featured in:

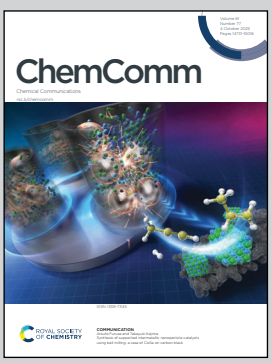

See Balamurugan Ramalingam *et al.*, *Chem. Commun.*, 2025, **61**, 14915.

ROYAL SOCIETY OF CHEMISTRY

rsc.li/chemcomm

Registered charity number: 207890

ChemComm

COMMUNICATION

View Article Online
View Journal | View Issue

Cite this: *Chem. Commun.*, 2025, **61**, 14915

Received 8th July 2025,
Accepted 14th August 2025

DOI: 10.1039/d5cc03841c

rsc.li/chemcomm

Electrochemical dehydrogenative intramolecular C–C coupling for expedient carbazole synthesis

Mingyue Wu,[a] Albertus Denny Handoko,[a] Kexin Zhu,[b] Chi-Lik Ken Lee,[a] Philip W. Miller,[b] Mark R. Crimmin[b] and Balamurugan Ramalingam *[ac]

An electrochemical method for carbazole synthesis *via* dehydrogenative aryl–aryl coupling of arylamines under metal-free conditions at ambient temperature is presented. The reactivity of arylamines is rationalised by cyclic voltammetry and density functional theory (DFT) studies to provide a preliminary understanding of the observed regioselectivity.

Dehydrogenative aryl–aryl coupling is a powerful strategy for constructing aromatic molecules by directly forming C–C bonds through oxidative processes.[1,2] Electrochemical dehydrogenative coupling uses the oxidation of suitable aromatic substrates to achieve the dimerisation of aryl units, providing a sustainable alternative to traditional metal-catalysed coupling reactions without chemical oxidants. When two aryl units are connected *via* a central nitrogen, intramolecular homo-coupling can occur, leading to the formation of carbazoles.[3] Carbazole derivatives are widely used in pharmaceuticals,[4] organic electronics,[5,6] and functional materials.[7,8] However, conventional carbazole synthesis often requires multiple reaction steps and suffers from poor atom economy. Thus, the electrochemical dehydrogenative coupling[9] of diphenylamine offers an efficient alternative solution for carbazole synthesis by reducing waste generation. This method eliminates the need for pre-functionalised feedstocks or external oxidants and the use of precious transition-metal catalysts, making it atom-efficient, environmentally benign and cost-effective.

Electrochemical dehydrogenative aryl–aryl coupling has been known for more than a decade, with significant progress reported for the synthesis of biphenols,[10–12] bianilides,[13] *meta*- and *para*-terphenyls, as well as cross-coupled products of various heterocycles with phenols.[14–16] However, the electrochemical dehydrogenative strategy has not been utilised for substrates that are pre-functionalised for carbazole synthesis. Transition metal-catalysed synthesis of carbazoles, involving oxidative pathways, has become increasingly attractive to conventional synthesis.[17–19] Three major approaches (Fig. 1) have been reported for the synthesis of carbazoles adopting novel methodologies: (i) concerted C–H activation of pre-functionalised bi-aryl amines and subsequent C–N bond formation *via* either amination (R = H, alkyl, Bn)[20] or amidation (R = acetyl)[21–23] using metal catalysts or electrochemical dehydrogenative coupling (Fig. 1a);[24] (ii) oxidative addition of aryl halides to metal catalysts followed by C–H activation (Fig. 1b),[25–30] (iii) intramolecular oxidative C–H/C–H coupling (Fig. 1c),[31,32] which can proceed in the presence of a metal catalyst or under photoredox conditions (*e.g.*, using Fe-[33] or Cu[34]-based catalysts) with iodine or molecular oxygen as the oxidant. While the above approaches are applicable to a broad range of substrates, the need for pre-functionalisation with either amines or halogens and the reliance on precious metals for substrate activation are disadvantageous. From a sustainability standpoint, metal-free strategies in organic synthesis are especially attractive compared to methods that depend on precious metal catalysis.

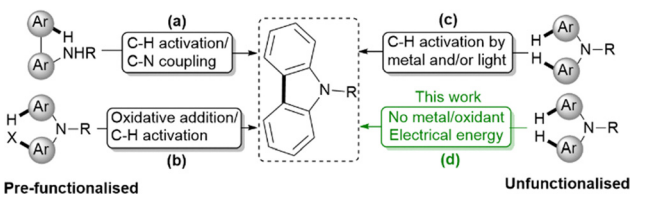

Fig. 1 Current attractive strategies (a)–(c) for the synthesis of carbazoles compared to our sustainable approach (d). Existing strategies (a)–(c) rely on metal catalysts or oxidants and require pre-functionalized substrates. In contrast, our sustainable approach (d) uses only electricity to achieve oxidative coupling of aryl groups at room temperature, eliminating the need for oxidants or metal catalysts.

[a] *Institute of Sustainability for Chemicals, Energy and Environment (ISCE²), Agency for Science, Technology and Research (A*STAR), 1 Pesek Road, Singapore 627833, Republic of Singapore. E-mail: balamurugan_ramalingam@isce2.a-star.edu.sg*

[b] *Molecular Sciences Research Hub, Department of Chemistry, Imperial College London, London, W12 0BZ, UK*

[c] *Institute of Materials Research and Engineering (IMRE), Agency for Science Technology and Research (A*STAR), Singapore 138634, Republic of Singapore*

To the best of our knowledge, neither simple nor substituted carbazoles have been synthesised from diaryl- or triaryl-amines *via* anodic oxidation without the use of oxidants, metals or photoredox catalysts. Notably, Beil *et al.*[35] reported oxidative coupling using an active molybdenum anode under a constant current density of 7.5 mA cm^{-2}. Under these conditions, the formation of six- or seven-membered rings was favoured, achieving isolated yields of up to 80%. It was proposed that $[Mo\{OCH(CF_3)_2\}_5]$, generated in the reaction medium, played a key role in promoting oxidative coupling. Nevertheless, the formation of carbazoles was limited to a yield of only 10%, and the synthesis of other five-membered rings remained challenging, with yields reaching up to 31%. Herein, we report an electrochemical method for carbazole synthesis carried out at room temperature, without the use of metal catalysts or external oxidants. This environmentally benign approach allows direct C–C bond formation without the use of metal catalysts. Furthermore, this study offers valuable insights into the underlying reaction pathways for the selective formation of carbazoles.

Electrochemical oxidation of tris(3,4-dimethoxyphenyl)amine (**A1**) was initiated in a two-electrode setup under galvanostatic control. A detailed optimisation study is presented in Table S1 (SI). The optimal conditions were then applied to various tertiary amines to explore the homo-aryl coupling reaction scope (Fig. 2). Highly electron-rich substrates like **A1** can undergo oxidation readily, affording the desired carbazole **C1** in 85% isolated yield. Replacing one of the OMe groups by a Me group as in **C2** or the 3,4-dimethoxyphenyl moiety by phenyl (**C3**) decreased the yield substantially. Replacing the electron-rich aryl rings of the tertiary aryl amine with a *p*-halo-substituted phenyl group did not significantly impact the product yields, affording carbazoles **C4–C6** in 61–89% yields. Notably, no dehalogenation or direct arylation of products was observed, which is one of the possible side reactions in metal-catalysed coupling reactions. Functional groups such as –CN (**C7**), –CHO (**C8**) and $-CO_2Me$ (**C9**) were unaffected under the electrooxidation conditions and provided the coupling products in good to excellent yields (61–84%). Notably, the stepwise replacement of the 3,4-dimethoxyphenyl groups with unsubstituted phenyl rings had a marked effect on the yields of **C3** (63%) and **C11** (0%). The optimised methodology appears to perform well with electron-rich substrates, and we believe there is significant potential to extend its applicability to electron-deficient substrates by fine-tuning the electrochemical conditions and by suppressing side reactions.

To understand the reactivity differences amongst substrates, cyclic voltammetry (CV) examinations were performed on **A1**, **A3**, and **A11** under the same reaction conditions using a potentiostat (Gamry Reference 600+). Three oxidation and reduction event pairs were detected, respectively, on **A1** upon the first anodic and return cathodic scans (Fig. 3a). The O_1/R_1 pair displayed a relatively symmetrical peak area ratio of ~0.91 and a moderate peak-to-peak separation (ΔE_p) of ~157 mV, indicative of a (quasi)reversible single electron transfer process (E_r).[36] Although the ΔE_p is wider than the theoretical value of 60 mV, it is comparable to that of a Fc/Fc^+ reference

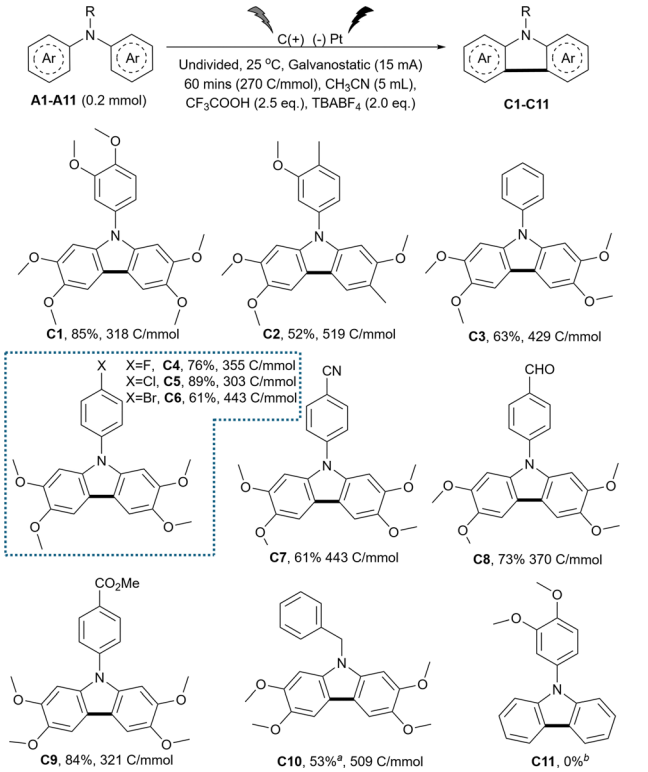

Fig. 2 Efficiency of electrochemical dehydrogenative coupling of tertiary amines. Isolated yields are reported. Refer to the SI for the synthesis of starting materials (**A1–A11**) and the corresponding products (**C1–C11**) and analytical data. [a] In the presence of 10 mol% of ferrocene as a mediator. [b] Possible formation of the dimerization product (**C11-dimer**, 38%) was observed (*cf.* SI, Section S6).

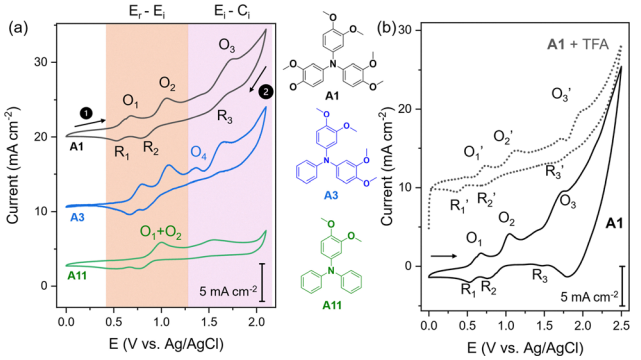

Fig. 3 Cyclic voltammetry (CV) was performed on a mirror polished glassy carbon working electrode (~0.071 cm^2), a platinum counter electrode (~2 cm^2), and a leakless Ag/AgCl reference electrode under the optimised reaction conditions described in Fig. 2 but with a larger total volume of 10 mL. (a) Cyclic voltammetry (CV) of **A1**, **A3** and **A11** at a scan rate of 10 mV s^{-1} *vs.* Ag/AgCl. (b) CV of **A1** before (solid line) and after TEA addition (dotted lines).

($\Delta E_p \approx 120$ mV, Fig. S2a), suggesting a significant influence of *iR* drop or passivation that widens ΔE_p. O_2/R_2 shows a more irreversible single electron transfer behaviour (E_i) with a larger peak area ratio of ~1.26 and a wider ΔE_p of ~278 mV. Distinct

from the rest, the O_3/R_3 pair is unsymmetrical, with a very large area ratio of >30 and a ΔE_p of $\sim$257 mV, indicative of a two-step reaction consisting of irreversible electron transfer followed by an irreversible chemical reaction (E_i–C_i). As the oxidative coupling process of **A1** to yield **C1** is expected to involve 2 e^- transfer, we hypothesise that the relevant coupling process is reflected by O_1 and O_2, while O_3 may be linked to overoxidation that could lead to possible side-reactions decreasing the efficiency of the coupling reaction.[37] Our position is supported by chronopotentiometric measurements of **A1** at 10 and 15 mA (5.6 and 8.5 mA cm^{-2}, respectively, Fig. S4), where a poor **C1** yield (12%) at 10 mA applied current (Table S1, entry 5) can be rationalised to the insufficient voltage ($\sim$0.7 V max) to reach the O_2 oxidation event.

Comparing the redox behaviour of different substrates, O_1 and O_2 peaks are 12–16 mV more anodic on **A3** (Fig. 3a), suggesting that the oxidative coupling of the latter is more arduous. **A3** also displays similar O_3 potential to **A1**. However, a new irreversible oxidation peak, O_4, was detected at 1.46 V, earlier than O_3. This suggests that **A3** may have additional overoxidation mechanisms that can adversely affect the **C3** yield (63%). The redox behaviour of **A11** (Fig. 3a) is rather different, with only two oxidation events, O_5 and O_3, observed in the potential range of CV. As reduction events R_1 and R_2 are still present around 0.50 and 0.76 V, we deduced that reduction event O_5 may represent merged O_1 and O_2 components. The position of the O_5 peak is at least 320 mV more anodic compared to O_1 in **A1**, suggesting that the oxidative coupling process on **A11** is more challenging. At the same time, the O_3 peak appears 250 mV earlier compared to **A1**, suggesting more facile overoxidation. We believe that the combination of these factors might lead to the formation of a possible dimeric product, **C11-dimer** (*cf.* Section S6, SI), rather than the expected **C11**.

Next, the role of the TFA additive can be elucidated by comparing the CV of **A1** with and without TFA (Fig. 3b). With TFA addition, the most notable change in the redox behaviour of **A1** is the anodic shift of the O_3 peak to O_3' from 1.76 to 1.96 V, while the positions of O_1' and O_2' are relatively unchanged from O_1 and O_2, barring a 4–6 mV shift. Thus, we posit that the TFA addition does not actually make the oxidative coupling of **A1** easier, but rather it makes the over-oxidation event more difficult through protonation of the central N atom. Thus, a more stable **A1** (or **C1**) would allow the current controlled coupling process to proceed with a wider electrochemical stability window. This hypothesis is corroborated by significantly ($\sim$5.9×) steeper yield growth compared to conversion growth with more TFA added (Fig. S4, SI). A relatively strong and electrochemically stable acid is required for this scheme, as our attempt to substitute TFA with acetic acid (Table S1, entry 10) did not improve the **C1** yield. On the other hand, more acidic methanesulfonic acid (Table S1, entry 8) appears to improve the **C1** yield slightly but not as good as TFA, possibly because of the better oxidation stability of TFA.[38]

In the electrochemical oxidation process, we observed the favourable formation of the C_6–$C_{6'}$ coupling products of carbazole. A plausible reaction pathway for the formation of

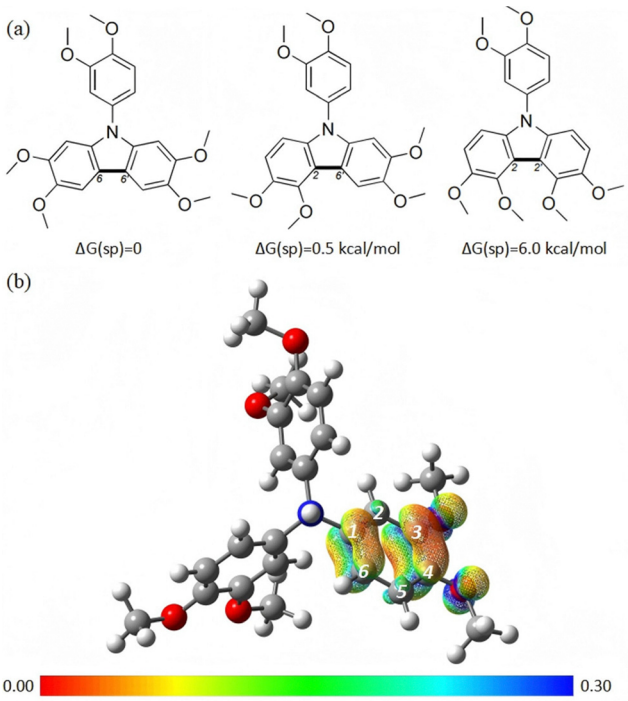

Fig. 4 DFT calculations were carried out using Gaussian 16 (Revision C.02). Geometry optimisation was performed using the ωB97X-D functional including geometrical dispersion corrections described by Grimme's D2 correction. (a) Structures of three different optimised isomers of **C1** (from left to right, C6–C6′, C2–C2′, and C2–C6′). (b) Spin density distribution of ^{2}[**A1-H**]$^{2+}$.

carbazole product **C1** is proposed in Fig. S9. To gain insight into the electronic and structural properties underlying the electrochemical dehydrogenative C–C coupling reaction, we employed density functional theory (DFT) calculations. These calculations focused on the relative energies of the isomeric forms of the products and the electronic structure of potential reaction intermediates. The Gibbs free energies of formation were calculated for the three possible oxidation products obtained through coupling at the C_2–$C_{2'}$, C_2–$C_{6'}$, and C_6–$C_{6'}$ carbon atoms of **A1** (Fig. 4a). A series of possible conformers for each product were identified based on the relative orientation of the methoxy groups with respect to their attached phenyl rings. The DFT analysis reveals that, among the various conformations, the lowest-energy structure corresponds to the C_6–$C_{6'}$ coupled product, which is thermodynamically more stable by 0.5 kcal mol^{-1} compared to the C_2–$C_{6'}$ product and by 6.0 kcal mol^{-1} compared to the C_2–$C_{2'}$ product. These data suggest that the selectivity of the reaction is determined by the low kinetic barrier to form the experimentally observed C_6–$C_{6'}$ product rather than thermodynamics.

To gain further insight into the electronic properties of potential reaction intermediates, the structures of the radical cation ^{2}[**A1**]$^+$ and its protonated analogue ^{2}[**A1-H**]$^{2+}$ were calculated defining each as a doublet spin state (S = 1/2). Given the experimental reaction conditions and high concentration of TFA, it is likely that the substrate exists in its protonated form in solution and ^{2}[**A1-H**]$^{2+}$ is a plausible intermediate following

electrochemical oxidation of $[\mathbf{A1\text{-}H}]^{+}$. Examination of the spin-density plot of $^{2}[\mathbf{A1\text{-}H}]^{2+}$ (Fig. 4b) shows that the unpaired electron's spin is confined within just one of the aryl rings. While delocalised, there is spin-density on the C_6 position, suggesting that this site should possess radical character and thereby supporting the experimentally observed site of reactivity.

In summary, this study presents an electrochemical approach for synthesising carbazoles *via* intramolecular dehydrogenative aryl–aryl coupling of arylamines. The methodology offers significant advantages in terms of atom economy, eliminating the need for precious metal catalysts, stoichiometric oxidants, or pre-functionalised starting materials. Trifluoroacetic acid (TFA) was identified as a critical additive, increasing the yield of **C1** from 29% to 87% by expanding the electrochemical stability window and suppressing undesired overoxidation. The method afforded good to excellent yields (61–90%) across a range of electron-rich and *para*-halo-substituted substrates, whereas less electron-donating groups led to a marked decrease in efficiency. The reaction exhibited complete regioselectivity, consistently yielding the C_6–$C_{6'}$ coupled product. DFT calculations supported the experimental observations, showing the observed product is the thermodynamically most stable isomer and is also likely kinetically favoured based on the electronic structure of the possible radical intermediate. Overall, this work establishes a practical and mechanistically informed method for carbazole synthesis and contributes to the advancement of methodologies in electroorganic synthesis. We are currently focusing on expanding the new methodology for the construction of oxygen- and sulphur-containing heterocycles, as well as the synthesis of carbazole-containing natural products.

This work was funded by the Horizontal Technology Coordinating Office (HTCO), Agency for Science, Technology and Research (A*STAR), Singapore, under project number C2312 18004. B. R. acknowledges the Materials Generative Design and Testing Framework (MAT-GDT) Program at A*STAR (Grant No. M24N4b0034) for the support.

Conflicts of interest

There are no conflicts to declare.

Data availability

Detailed electrochemical studies, DFT calculations and NMR spectral data for this article have been included as part of the SI. See DOI: **https://doi.org/10.1039/d5cc03841c**

Notes and references

1 J. L. Röckl, D. Pollok, R. Franke and S. R. Waldvogel, *Acc. Chem. Res.*, 2020, **53**, 45–61.
2 Y. Yuan and A. Lei, *Acc. Chem. Res.*, 2019, **52**, 3309–3324.
3 L. A. T. Allen and P. Natho, *Org. Biomol. Chem.*, 2023, **21**, 8956–8974.
4 A. Caruso, J. Ceramella, D. Iacopetta, C. Saturnino, M. V. Mauro, R. Bruno, S. Aquaro and M. S. Sinicropi, *Molecules*, 2019, **24**, 1912.
5 Y. Liu, Y. Sun, M. Li, H. Feng, W. Ni, H. Zhang, X. Wan and Y. Chen, *RSC Adv.*, 2018, **8**, 4867–4871.
6 M. Li, W. Ni, H. Feng, X. Wan, Y. Liu, Y. Zuo, B. Kan, Q. Zhang and Y. Chen, *Org. Electron.*, 2015, **24**, 89–95.
7 X.-D. Yuan, J. Liang, Y.-C. He, Q. Li, C. Zhong, Z.-Q. Jiang and L.-S. Liao, *J. Mater. Chem. C*, 2014, **2**, 6387.
8 D. Magaldi, M. Ulfa, S. Péralta, F. Goubard, T. Pauporté and T.-T. Bui, *J. Mater. Sci.: Mater. Electron.*, 2021, **32**, 12856–12861.
9 A. B. Dapkekar, J. Naveen and G. Satyanarayana, *Asian J. Org. Chem.*, 2025, **14**, e202500324.
10 B. Dahms, P. J. Kohlpaintner, A. Wiebe, R. Breinbauer, D. Schollmeyer and S. R. Waldvogel, *Chem. – Eur. J.*, 2019, **25**, 2713–2716.
11 B. Elsler, D. Schollmeyer, K. M. Dyballa, R. Franke and S. R. Waldvogel, *Angew. Chem., Int. Ed.*, 2014, **53**, 5210–5213.
12 B. Elsler, A. Wiebe, D. Schollmeyer, K. M. Dyballa, R. Franke and S. R. Waldvogel, *Chem. – Eur. J.*, 2015, **21**, 12321–12325.
13 L. Schulz, M. Enders, B. Elsler, D. Schollmeyer, K. M. Dyballa, R. Franke and S. R. Waldvogel, *Angew. Chem., Int. Ed.*, 2017, **56**, 4877–4881.
14 A. Wiebe, S. Lips, D. Schollmeyer, R. Franke and S. R. Waldvogel, *Angew. Chem., Int. Ed.*, 2017, **56**, 14727–14731.
15 S. Lips, D. Schollmeyer, R. Franke and S. R. Waldvogel, *Angew. Chem., Int. Ed.*, 2018, **57**, 13325–13329.
16 S. Lips, B. A. Frontana-Uribe, M. Dörr, D. Schollmeyer, R. Franke and S. R. Waldvogel, *Chem. – Eur. J.*, 2018, **24**, 6057–6061.
17 D.-Y. Goo and S. K. Woo, *Org. Biomol. Chem.*, 2016, **14**, 122–130.
18 T. Watanabe, S. Oishi, N. Fujii and H. Ohno, *J. Org. Chem.*, 2009, **74**, 4720–4726.
19 D. J. St. Jean, S. F. Poon and J. L. Schwarzbach, *Org. Lett.*, 2007, **9**, 4893–4896.
20 J. A. Jordan-Hore, C. C. C. Johansson, M. Gulias, E. M. Beck and M. J. Gaunt, *J. Am. Chem. Soc.*, 2008, **130**, 16184–16186.
21 W. C. P. Tsang, N. Zheng and S. L. Buchwald, *J. Am. Chem. Soc.*, 2005, **127**, 14560–14561.
22 S. H. Cho, J. Yoon and S. Chang, *J. Am. Chem. Soc.*, 2011, **133**, 5996–6005.
23 W. C. P. Tsang, R. H. Munday, G. Brasche, N. Zheng and S. L. Buchwald, *J. Org. Chem.*, 2008, **73**, 7603–7610.
24 A. Kehl, N. Schupp, V. M. Breising, D. Schollmeyer and S. R. Waldvogel, *Chem. – Eur. J.*, 2020, **26**, 15847–15851.
25 R. B. Bedford and C. S. J. Cazin, *Chem. Commun.*, 2002, 2310–2311.
26 K. K. Gruner and H.-J. Knölker, *Org. Biomol. Chem.*, 2008, **6**, 3902–3904.
27 D. Tsvelikhovsky and S. L. Buchwald, *J. Am. Chem. Soc.*, 2010, **132**, 14048–14051.
28 A. Khan, R. Karim, H. Dhimane and S. Alam, *ChemistrySelect*, 2019, **4**, 6598–6605.
29 Y. Tanji, N. Mitsutake, T. Fujihara and Y. Tsuji, *Angew. Chem., Int. Ed.*, 2018, **57**, 10314–10317.
30 L.-C. Campeau, M. Parisien, A. Jean and K. Fagnou, *J. Am. Chem. Soc.*, 2006, **128**, 581–590.
31 G. Brufani, S. Chen, B. Di Erasmo, A. Afanasenko, Y. Gu, C.-J. Li and L. Vaccaro, *ACS Sustainable Chem. Eng.*, 2024, **12**, 8562–8572.
32 S. Trosien, P. Böttger and S. R. Waldvogel, *Org. Lett.*, 2014, **16**, 402–405.
33 S. Parisien-Collette, A. C. Hernandez-Perez and S. K. Collins, *Org. Lett.*, 2016, **18**, 4994–4997.
34 A. C. Hernandez-Perez and S. K. Collins, *Angew. Chem., Int. Ed.*, 2013, **52**, 12696–12700.
35 S. B. Beil, T. Müller, S. B. Sillart, P. Franzmann, A. Bomm, M. Holtkamp, U. Karst, W. Schade and S. R. Waldvogel, *Angew. Chem., Int. Ed.*, 2018, **57**, 2450–2454.
36 R. S. Nicholson, *Anal. Chem.*, 1965, **37**, 1351–1355.
37 K. Karon and M. Lapkowski, *J. Solid State Electrochem.*, 2015, **19**, 2601–2610.
38 C. Depecker, H. Marzouk, S. P. Trevin and J. Devynck, *New J. Chem.*, 1999, **23**, 739–742.

